Steady State Phenol Degradation in a Draft-Tube, Gas-Liquid-Solid Fluidized-Bed Bioreactor

Experiments on phenol biodegradation by a mixed culture in a draft-tube, three-phase fluidized-bed biofilm reactor (DTFBR) at the steady state were performed. The characteristics of biofilms developed in the DTFBR were identified. A steady state biofilm model was proposed that considers the simultaneous diffusion and reaction of oxygen and phenol within the biofilm and the external mass transfer resistance between the biofilm and the completely mixed bulk liquid phase. The proposed model assumes a double-substrate limiting mechanism for microbial growth kinetics, and Haldane and Monod type expressions were used to characterize the dependence of microbial specific growth rate on phenol and oxygen, respectively. The experimental results were used to test the validity of the proposed model.

Wen-Tzung Tang, Liang-Shih Fan
Department of Chemical Engineering
Ohio State University
Columbus, OH 43210

Introduction

Recently, fluidized-bed bioreactors have received increasing interest and wide utilization in both fermentation processes and wastewater treatment. The fluidized-bed biofilm reactor has been demonstrated to outperform other reactor configurations used in wastewater treatment such as the activated sludge system and packed-bed (or trickling-filters) bioreactor by Holladay et al. (1978) and Lee et al. (1979).

The superior performance of the fluidized-bed bioreactor stems from the following factors:

1. Very high biomass concentration up to 30–40 kg/m^3 can be achieved due to immobilization of cells onto or into the solid particles.
2. The limit on the operating liquid flow rates imposed by the microbial maximum specific growth rate as encountered in the continuous stirred-tank reactor system is eliminated due to the decoupling of the residence time of the liquid phase and of the microbial cells.
3. Intimate contact between the liquid phase and solid phase is achieved.
4. The use of supporting particles allows the partial replenishment of the fluidized bed without interrupting the operation in order to maintain high microbial activity.

Correspondence concerning this paper should be addressed to Liang-Shih Fan.

(Dunn et al., 1983; Scott and Hancher, 1976; Atkinson et al., 1984)

Modeling of a solid-liquid, two-phase fluidized-bed biofilm reactor has been attempted by several investigators (Shieh, 1980; Stathis, 1980; Mulcahy et al., 1981; Ying and Weber, 1979; Jennings et al., 1976; Wang and Chi, 1984). The microbial growth kinetics considered in the above models were of either zero order or first order, or Monod equation. The situation in which oxygen can become the limiting substrate inside the biofilm was not considered in the above models (except Stathis, 1980), and most of them assumed negligible external mass transfer resistance between the biofilm and bulk liquid phase.

In aerobic wastewater treatment systems, especially those dealing with toxic but biodegradable organics such as phenolic compounds, the microbial growth kinetics can be best described by a substrate inhibiting mechanism. A model based on the Monod equation, or the zero- or first-order reaction kinetics will not be applicable. In the cases of thick biofilm, high substrate concentration, or low bulk oxygen concentration, an oxygen-limiting situation could be encountered, and should be included in the biofilm model. Finally, external mass transfer resistance may not be negligible for systems with a reaction rate comparable to or higher than the external mass transfer rate. A more general steady state biofilm model—one that considers a double-substrate (oxygen and an inhibitory substrate) limiting

kinetics, internal diffusion of substrates and oxygen within the biofilms, and external mass transfer resistance between the biofilms and completely mixed bulk liquid phase—was proposed in this study. Experiments of phenol biodegradation in a draft-tube, three-phase fluidized-bed biofilm reactor were performed to test the validity of the proposed model.

Model Development

In a draft-tube, three-phase fluidized-bed bioreactor (DTFBR) the pressure difference between the draft and annular regions drives a complete circulation of liquid and solid phases between these two regions. The turbulence created by the direct injection of gas bubbles into the draft tube of the reactor leads to an intimate contact between the liquid and solid phases. In addition, the liquid circulation time differs from the liquid mean residence time by an order of magnitude. Consequently, the assumption that a complete mixing state is achieved in the DTFBR is a reasonable approximation, as demonstrated by Hwang and Fan (1985).

The biodegradation of phenol in the biofilms immobilized on activated carbon particles contained in the DTFBR, under pseudosteady state, consists of the following basic processes:

1. Transport of oxygen from gas phase into liquid phase
2. Transport of phenol, other nutrients, and oxygen from bulk liquid phase to the surfaces of biofilms
3. Simultaneous diffusion and reaction of phenol, other nutrients, and oxygen within the biofilms

A pseudosteady state is reached in the completely mixed draft-tube, three-phase fluidized-bed biofilm reactor when the bulk concentrations of phenol and oxygen are constant, and the change in biofilm properties such as biofilm thickness and density are negligible. Consequently, the concentration profiles of phenol and oxygen within the biofilms are invariant with respect to time, and these concentration profiles within the activated carbon particles are flat. The pseudosteady state also implies that the growth of biomass on the biofilm is instantaneously sloughed off by fluid shear and particle-particle abrasion such that biofilm thickness and overall biofilm density remain constant.

Based on the complete mixing and the pseudosteady state (steady state, for simplicity hereafter) approximations, the concentrations of phenol and oxygen in the bulk liquid phase in the DTFBR can be described by the following mass conservation equations:

$$Q(S^i - S^b) - k_s A_b(S^b - S^s) = 0 \tag{1}$$

$$Q(C^i - C^b) + K_l a V_R(C^e - C^b) - k_c A_b(C^b - C^s) = 0 \tag{2}$$

The external mass transfer resistance between the liquid phase and the surfaces of biofilms has been regarded as negligible in most of the modeling for fluidized-bed bioreactors (Wang and Chi, 1984; Ying and Weber, 1979; Park et al., 1984; Mulcahy et al., 1981). However, whether the external mass transfer resistance is negligible or not strongly depends upon the relative rate of external mass transfer to that of bioreaction of the biofilm, which in turn is affected by the size of the bioparticle and the biofilm density. Consequently, the assumption of negligible external mass transfer resistance needs to be carefully evaluated for every specific biofilm system. In the present system, the external liquid-solid mass transfer coefficient of phenol, k_s, was obtained as 0.004 cm/s experimentally using the benzoic acid dissolution method. Using this k_s value and Eq. 1, the phenol concentrations at the biofilm surface, S^s, were calculated as tabulated in Table 3. Comparison of the S^s and S^b shows that the concentration gradients of phenol in the liquid film surrounding the biofilms account for more than 20% of the bulk phenol concentrations in this study. Larger than 15% error in phenol biodegradation rate will be obtained if the external liquid-solid mass transfer resistance is neglected. Consequently, the external mass transfer effect must be included in the model.

The overall rates of phenol biodegradation and oxygen consumption, R_v and R_{ov}, respectively, are given by:

$$R_v = k_s A_b(S^b - S^s) = \left[\frac{V_R(1 - \epsilon_l - \epsilon_g)}{\left(\frac{4}{3}\right)\pi r_f^3}\right] 4\pi r_f^2 D_{s,f} \left.\frac{dS}{dr}\right|_{r=r_f} \tag{3}$$

and

$$R_{ov} = k_c A_b(C^b - C^s) = \left[\frac{V_R(1 - \epsilon_l - \epsilon_g)}{\left(\frac{4}{3}\right)\pi r_f^3}\right] 4\pi r_f^2 D_{c,f} \left.\frac{dC}{dr}\right|_{r=r_f} \tag{4}$$

Equations 3 and 4 assume that the consumption of both phenol and oxygen by the bioflocs sloughed off from the bioparticles and suspended in the bulk liquid phase is negligible as compared to the consumption by the biofilms. Solution of Eqs. 3 and 4 requires knowledge of the concentration profiles of phenol and oxygen within the biofilms. These profiles are governed by the diffusional flux of phenol and oxygen through the biofilm and the reaction kinetics of the consumption of both phenol and oxygen by cells constituting the biofilms. Formulation of such a biofilm model is based on the following assumptions:

1. The activated carbon particles are spherical in shape and uniform in size.
2. The microorganisms are uniformly distributed over the surface of activated carbon particles forming a uniform biofilm. The bioparticles (i.e., activated carbon covered with biofilm) are assumed to be spherical in shape. Although there exists a size distribution, the size of these bioparticles can be well represented by their average diameter.
3. The various species of microbes present in the biofilm can be treated as a single imaginary species. Accordingly, the biological parameters used to depict the activity of a pure culture can be employed to describe the metabolic activity of such an imaginary species.
4. The biofilm is treated as a homogeneous phase within which phenol and oxygen diffuse and are consumed.
5. The growth-limiting nutrients are phenol and oxygen. All other nutrients are present in excess.
6. There is no physiological change of the microbes when immobilized onto the activated carbon particles, so that the kineitc expressions of cell growth and substrate degradation obtained from a suspended cell culture can be applied equally well to the immobilized system.
7. The effects of the outward diffusion of metabolic products are negligible.
8. The diffusivities of phenol and oxygen in the biofilm are

assumed to be constant, independent of the radial position in the biofilm and of the concentrations of phenol and oxygen for a given biofilm thickness.

9. The growth kinetic expressions on phenol and oxygen concentrations are assumed to follow the following relationship:

$$\mu = \frac{\mu_{max} S}{K_s + S + S^2/K_i} \frac{C}{K_{ox} + C} \tag{5}$$

In Eq. 5, the dependence of the growth kinetics on phenol and oxygen concentrations is assumed to follow the Haldane-type function and Monod equation, respectively.

10. The effects of bioadsorption of both phenol and oxygen are negligible. Based on the above assumptions, the simultaneous transport and consumption of phenol and oxygen within the biofilm can be described from macroscopic mass conservation as:

$$\frac{D_{s,f}}{r^2}\left[\frac{d}{dr}\left(r^2 \frac{dS}{dr}\right)\right] - \frac{\rho_v}{Y_{x/s}} \frac{\mu_{max} S}{S + K_s + S^2/K_i} \frac{C}{K_{ox} + C} = 0 \tag{6}$$

$$\frac{D_{c,f}}{r^2}\left[\frac{d}{dr}\left(r^2 \frac{dC}{dr}\right)\right] - \frac{\rho_v}{Y_{x/o}} \frac{\mu_{max} S}{S + K_s + S^2/K_i} \frac{C}{K_{ox} + C} = 0 \tag{7}$$

The $Y_{x/s}$ and $Y_{x/o}$ in Eqs. 6 and 7 are the observed yield coefficients for phenol and oxygen, respectively. The specific rate of substrate utilization for cell maintenance is usually very small as compared with the specific growth rate in the logarithmic growth phase, and is assumed to be negligible in Eqs. 6 and 7.

The corresponding boundary conditions for Eqs. 6 and 7 are given as:

$$\frac{dS}{dr} = 0 \quad \text{at } r = r_p \tag{8}$$

$$\frac{\partial C}{\partial r} = 0 \quad \text{at } r = r_p \tag{9}$$

and

$$D_{s,f} \frac{dS}{dr} = k_s (S^b - S^s) \quad \text{at } r = r_p + \delta \tag{10}$$

$$D_{c,f} \frac{dC}{dr} = k_c (C^b - C^s) \quad \text{at } r = r_p + \delta \tag{11}$$

Equations 6 and 7 and their boundary conditions can be expressed in dimensionless forms as:

$$\frac{d^2 S^*}{d\xi^2} + \frac{2}{\xi}\frac{dS^*}{d\xi} - \phi_s \frac{S^*}{K_s^* + S^* + (S^*)^2/K_i^*} \frac{C^*}{K_{ox}^* + C^*} = 0 \tag{12}$$

$$\frac{d^2 C^*}{d\xi^2} + \frac{2}{\xi}\frac{dC^*}{d\xi} - \phi_{ox} \frac{S^*}{K_s^* + S^* + (S^*)^2/K_i^*} \frac{C^*}{K_{ox}^* + C^*} = 0 \tag{13}$$

and

Boundary condition I:

$$\frac{dS^*}{d\xi} = \frac{dC^*}{d\xi} = 0 \quad \text{at } \xi = 1 \tag{14}$$

Boundary condition II:

$$\frac{dS^*}{d\xi} = \frac{Bi_s}{2}\left(\frac{S^b}{S^s} - 1\right) \quad \text{at } \xi = 1 + \frac{\delta}{r_p} \tag{15}$$

$$\frac{dC^*}{d\xi} = \frac{Bi_{ox}}{2}\left(\frac{C^b}{C^s} - 1\right) \quad \text{at } \xi = 1 + \frac{\delta}{r_p} \tag{16}$$

where

$$\xi = r/r_p; \quad S^* = S/S^s; \quad C^* = C/C^s$$

$$K_s^* = K_s/S^s; \quad K_i^* = K_i/S^s; \quad K_{ox}^* = K_{ox}/C^s$$

$$\phi_s = \frac{\rho_v \mu_{max} r_p^2}{Y_{x/s} S^s D_{s,f}}; \quad \phi_{ox} = \frac{\rho_v \mu_{max} r_p^2}{Y_{x/o} C^s D_{c,f}};$$

$$Bi_s = \frac{k_s d_p}{D_{s,f}}; \quad Bi_{ox} = \frac{k_c d_p}{D_{c,f}};$$

Equations 12 to 16 can be solved provided the bulk concentrations of both phenol and oxygen, S^b and C^b, are known. Since S^b and C^b are coupled between the bioparticle phase and bulk liquid phase, a trial-and-error procedure is required to solve Eqs. 1, 2, 6, and 7, provided that the outlet phenol concentration is to be predicted from the above model.

Numerical method

A set of boundary-value ordinary differential equations, Eqs. 12–16, were solved using the finite-difference method. The resultant difference equations comprise a system of nonlinear, implicit algebraic equations. Powell's hybrid method and FORTRAN subroutine (Powell, 1970a, b) which combines the merits of the steepest descent method and Broyden's quasi-Newton method, was used to solve these nonlinear algebraic equations. The convergence criterion used for solution of the set of nonlinear difference equations is 10^{-5}.

Experimental

Equipment

The reaction kinetics of phenol degradation in biofilms was studied in a draft-tube, three-phase fluidized-bed bioreactor with a working volume of 1,000 cm^3. A diagram of the reactor is shown in Figure 1. The DTFBR was made of Plexiglas and was constructed of a detachable draft tube concentrically placed in a 7.6 cm ID, 35 cm high column. The draft tube consisted of three sections. The bottom section had an ID of 5.0 cm and a length of 3.0 cm; the contraction region was tapered at an angle of 60° and had a length of 1.45 cm; the upper section was a straight tube of 2.5 cm ID and 18 cm length. The bottom section of the DTFBR had a conical configuration with an angle of 45° to avoid a dead zone. A gas injector placed at the bottom of the conical section was made of a 3.81 cm ID Plexiglas tube topped

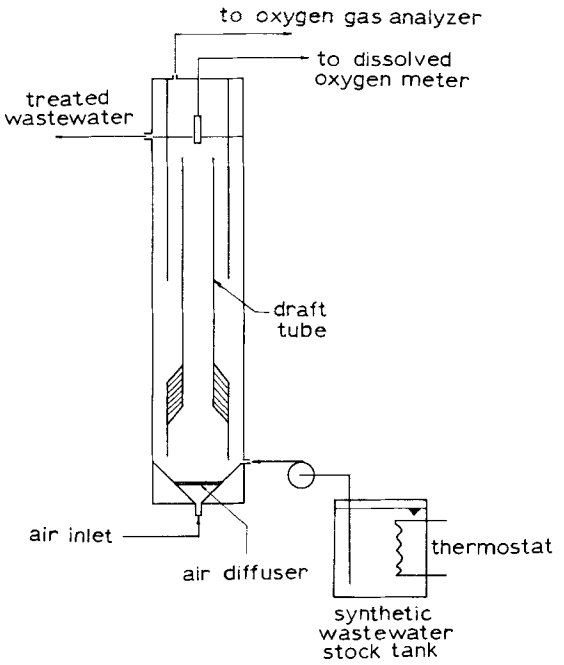

Figure 1. Diagram of 1,000 cm³ DTFBR.

with a porous plate of poly(methyl methacrylate) (PMMA). The average pore size of the PMMA plate is 15 μm.

The flow modes of a draft-tube, gas-liquid-solid fluidized-bed reactor can generally be classified into packed-, fluidized-, and circulated-bed modes, depending upon liquid and gas velocities employed (Fan et al., 1984). In this study, the DTFBR was operated under the circulated-bed mode in which both liquid and solid phases completely circulate between the draft and annular regions. The lower expanded section in the draft tube shown in Figure 1 was designed to prevent bypass of gas bubbles from the injector to the annular region. Since this section is far shorter than the upper straight section of the draft tube, its effect on the nature of completely mixed flow behavior of the DTFBR can be neglected.

Microbial culture and culture medium

Heterogeneous populations of microorganisms were obtained from the sewage lines in a coal conversion plant. The mixed culture was then conditioned to a synthetic wastewater containing phenol as the sole carbon and energy source, and was cultivated in a biooxidation tank for use in seeding the DTFBR. The composition of the synthetic stock feed solution is shown in Table 1. The stock solution was diluted to yield the desired phenol concentration for individual experimental runs.

Table 1. Composition of Synthetic Wastewater

Phenol	2.0	kg/m³
Ammonium nitrate	0.578	kg/m³
Phosphoric acid, 85%	120	cm³/m³
Ammonium chloride	0.006	kg/m³
Trace metals*	—	—
Ammonium hydroxide	added to adjust pH to 8.5	

*Trace metals include, g/m³: zinc 0.01, boron 0.02, molybdenum 0.01, manganese 0.01, copper 0.01, iron 0.01.

Biofilm thickness and dry density

The thickness of the biofilm was measured on an Olympus microscope (model BH-2) equipped with a Bausch & Lomb dial micrometer. The bioparticles appeared nearly spherical. For better representation of the size of the bioparticles, the largest and the smallest dimensions of each bioparticle were measured and the geometric mean was taken. At least 40 bioparticles were sampled and measured in each experimental run.

The dry biofilm density is expressed in terms of the dry weight of biomass of the biofilm per unit volume of wet biofilm. The wet biofilm volume was calculated based on the activated carbon diameter and the average biofilm thickness determined from microscopic examination. To determine the dry biomass, W, of the biofilm, the weight of dried cell mass plus that of the activated carbon particles was first obtained by drying the sample bioparticles at 105°C for 24 h. The biofilms were then removed from the carbon particles by heating the dried bioparticles in 0.25 M NaOH solution, with frequent microscopic examination until the biofilm was removed completely. The clean carbon particles were then washed with distilled water several times, dried at 105°C for 24 h, and weighted. Repeating the heating, washing, and drying processes on bare activated carbon particles showed negligible loss of mass. The dry biomass weight was then obtained by subtracting the weight of dried carbon particles from the weight of dried bioparticles. The biofilm dry density was calculated based on the following equation:

$$\rho_v = \frac{W}{N(\pi/6)\left[(d_p + 2\delta)^3 - d_p^3\right]} \tag{17}$$

where ρ_v is the biofilm dry density, d_p the average diameter of carbon particles, N the total number of carbon particles in the sample, and δ the average biofilm thickness. The total number of carbon particles in the sample was calculated by dividing the dry weight of clean carbon particles in the sample by the average weight of a single carbon particle, which was 0.0133 mg obtained from the average of 500 activated carbon particles in this study.

Phenol assay

Phenol was measured by a direct photometric method according to *Standard Methods* (1975). In this method, phenol was rapidly condensed with 4-aminoantipyrine, followed by oxidation with potassium ferricyanide at pH 10 to yield an amber-to-red compound. The absorbance of the resulting colored compound was measured at 510 nm using a Bausch & Lomb Spectrophotometer (model Spectronic 80).

Growth kinetics of phenol degrading suspended mixed culture

Growth kinetics data of the mixed culture were obtained from batch culture runs. The shake flask method was used to study the specific growth rates of the mixed culture at different phenol concentrations. In this experiment, 2.5 cm³ of tertiary subculture were used to inoculate 250 cm³ shake flasks containing 50 cm³ of medium of different initial phenol concentrations. The flasks were incubated at 23°C on a New Brunswick reciprocal shaker. The specific growth rates were determined graphically from linear semilogarithmic graphs of six to eight points.

Yield coefficients

The value of the observed yield coefficient $Y_{x/s}$, was determined according to the procedure given by Rittmann and McCarty (1980). A small inoculum consisting of approximately 0.12 kg/m^3 phenol and the other nutrients in proportions as specified in Table 1 was added to a 500 cm^3 flask. The contents were mixed vigorously with a magnetic stirrer. After the optical density of the inoculated culture reached its peak, the experiment was stopped and phenol concentration was assayed. The $Y_{x/s}$ was calculated as grams of cell mass increase per gram of phenol consumed.

The observed yield coefficient, $Y_{x/o}$, was indirectly determined in this study. The amount of oxygen per gram of phenol consumed, $Y_{o/s}$, was measured by an off-gas composition analysis technique using a Beckman model 755 oxygen gas analyzer and a YSI model 54ARC dissolved oxygen meter and probe, following the procedures given by Kubota et al. (1981). The value of $Y_{x/o}$ can then be calculated by dividing $Y_{x/s}$ by $Y_{o/s}$.

Experimental runs

Four steady state biofilm cultures were developed in the 1,000 cm^3 DTFBR. The operating conditions for each run are shown in Table 2; they include the influent phenol concentration, inlet liquid flow rate, bulk phenol and dissolved oxygen concentrations, volume fraction of bioparticles, superficial inlet gas flow rates, operating temperature, and pH.

Results and Discussion

Evaluation of biokinetic parameters

The specific growth rates of the mixed culture at different phenol concentrations were determined from the slopes of the linear semilogarithmic plots of the biomass concentration vs. the elapsed time in the initial exponential growth phase. By restricting the initial biomass concentration to very low values, changes in the initial medium composition were small when the initial exponential growth of the cultures began. The specific growth rates thus obtained were fitted by the Haldane equation using a nonlinear least-squares method. The fit of the Haldane equation is shown in Figure 2. The growth kinetic parameters derived were: $\mu_{max} = 0.365\ h^{-1}$, $K_s = 10.948 \times 10^{-3}$ kg/m^3, and $K_i = 113.00 \times 10^{-3}$ kg/m^3. These numerical values are very close to those reported in literature for mixed cultures growing on phenol (D'Adamo et al, 1984; Szetela and Winnicki, 1981; Pawlowsky and Howell, 1973).

Table 2. Operating Conditions in Steady State Experimental Runs

	Run No.			
	1	2	3	4
Liquid flow rate $\times 10^3$, m^3/h	2.01	2.3	2.3	2.01
Gas flow rate $\times 10^2$, m^3/h	8.5	8.5	8.5	8.5
Inlet phenol conc. $\times 10^3$, kg/m^3	38.09	49.17	96.20	72.71
Bulk phenol conc. $\times 10^3$, kg/m^3	2.69	3.50	6.49	3.54
Bulk dissolved oxygen conc. $\times 10^3$, kg/m^3	8.4	8.1	7.1	5.1
Temperature, °C	22–23	22–23	22–23	22–23.8
pH	6.9	6.8	6.9	6.9
Vol. frac. of bioparticles	0.048	0.049	0.064	0.080

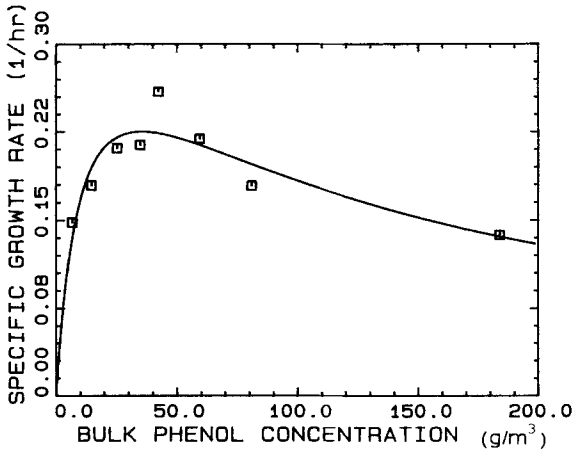

Figure 2. Specific growth rate of suspended mixed culture vs. phenol concentration.

□ experimental data; — result described by Haldane equation with kinetic constants $\mu_{max} = 0.365\ h^{-1}$, $K_s = 10.948$ g/m^3, $K_i = 113.004$ g/m^3

The double-substrate limiting kinetics used in the biofilm model assumes that phenol and oxygen are limiting substrates. The oxygen can become the limiting substrate only when the local oxygen concentration inside the biofilm is lower than the critical oxygen concentration (minimum oxygen concentration at individual cell surface to give maximum oxygen uptake rate). Such a situation occurs when the biofilm is very thick, or phenol concentration is high, or oxygen concentration is very low.

The critical oxygen concentration was not determined in this study, nor the K_{ox}. The critical oxygen concentrations for microorganisms generally lie in the range from 0.096×10^{-3} to 1.6×10^{-3} kg/m^3, and the saturation constant for oxygen, K_{ox}, is about one-third that of the critical oxygen concentration (Bailey and Ollis, 1977). Bacteria usually have lower values of critical oxygen concentration and K_{ox}. The values of K_{ox} for microorganisms compiled by Atkinson and Mavituna (1983) showed that most of the bacteria have a K_{ox} value less than 0.1×10^{-3} kg/m^3. Since the predominant organisms forming the dense biofilm in this study were bacteria mainly belonging to *Pseudomonas*, a value of 0.1×10^{-3} kg/m^3 was chosen for K_{ox} in the subsequent simulation.

The averaged yield coefficients, $Y_{x/s}$, and the amount of oxygen per gram of phenol consumed, $Y_{o/s}$, obtained from this study were 0.496 mg cell/mg phenol and 1.4 mg O_2/mg phenol, respectively. The growth yield coefficient, $Y_{x/s}$, reported in literature ranged from 0.45 to 0.85 for both pure and mixed cultures growing on phenol (Yang and Humphrey, 1975; Hill and Robinson, 1975; Jones et al., 1973; Pawlowsky and Howell, 1973; Beltrame et al., 1980). The values of $Y_{o/s}$ were 1.36 mg/mg for pure culture of *Candida tropicalis* reported by Klein et al. (1979) and 1.231 mg/mg for mixed culture obtained by Suzuki et al. (1983). Theoretically, complete oxidation of 1 mol phenol requires 7 mol oxygen, which corresponds to a value of 2.38 mg O_2/mg phenol. Since biomass grows on phenol as well, the apparent $Y_{o/s}$ is supposedly lower than 2.38 mg O_2/mg phenol. It is also possible that phenol was not completely degraded, as suggested by Klein et al. in their system.

The biofilm thicknesses and biofilm dry densities corresponding to the four steady state runs are shown in Table 3. The biofilm dry density seemed to decrease with increasing biofilm thickness. Variations of biofilm dry density with biofilm thickness have been reported with slightly different characteristics by Hoehn and Ray (1973), Shieh et al. (1981), and Timmermans and Van Haute (1984). It seems that variation of biofilm dry density with biofilm thickness strongly depends upon the species of microorganisms forming the biofilms, the substrate loading rates, and the reactor configuration and operating conditions in which the biofilms are cultivated. The biofilm dry densities obtained in this study have higher values than those obtained from two-phase fluidized-bed systems. This is probably due to the fact that cells in the biofilms developed in the DTFBR have to pack more tightly and closer together to resist the considerably higher shear existing in this three-phase system. The higher dry density of the biofilms at a given biofilm thickness obtained in the DTFBR will yield a higher biomass holdup in the reactor for a given solid particle loading.

Estimation of diffusivities of phenol and oxygen within the biofilm

The substrates and oxygen diffusivities through biofilms or aggregated bioflocs have been experimentally measured and reported to range from 2 to 90% of the diffusivities in pure water system (Bungay et al., 1969; Mueller et al., 1968; Williamson and McCarty, 1976; Smith and Coackley, 1984; Matson and Characklis, 1976). It appears that the diffusivities of substrates and oxygen within the biofilms or bioflocs strongly depend upon physical and biological characteristics such as the density and thickness of the biofilms or bioflocs. Since the characteristics of biofilms vary with operating or cultivation conditions, experimental determination of these diffusivities for biofilms obtained from different operating conditions would become very difficult. This study therefore resorted to an indirect method to obtain the diffusivities of phenol and oxygen within the biofilm. Since in the proposed steady state model the diffusivities of substrate and oxygen within biofilms are the only unknown parameters, they can be evaluated by adjusting their numerical values to give the best fit of the volumetric biofilm phenol degradation rates predicted from integrating the local phenol degradation rate over the biofilm in a single bioparticle as given by Eq. 18 to those calculated from experimental data according to Eq. 19.

$$r_{sv} = \frac{\int_{r_p}^{r_f} \frac{\rho_v}{Y_{x/s}} \frac{\mu_{\max} S}{K_s + S + S^2/K_i} \frac{C}{K_{ox} + C} 4\pi r^2 \, dr}{\frac{4}{3}\pi (r_f^3 - r_p^3)} \tag{18}$$

$$r_{sv} = \frac{Q(S^i - S^b)}{V_b} \tag{19}$$

The results are shown in Table 3 with the diffusivities of phenol and oxygen expressed as the fraction of those in pure water at 23°C, which are 0.033 and 0.0828 cm²/h, respectively. It should be noted that the assumed value of K_{ox} in the biofilm model has little effect on the results of the diffusivities evaluation, for the bulk dissolved oxygen concentrations in the four steady state runs were sufficiently high, as shown in Table 2, and the biofilms were thin, Table 3, such that the oxygen limiting condition was not encountered.

Table 3. Diffusivity of Phenol at Different Biofilm Thicknesses

δ μm	ρ_v mg/cm³	$S^b \times 10^3$ kg/m³	$S^s \times 10^3$ kg/m³	D_f/D_w	$(r_{sv})_{exp}$ mg/cm³ · h	$(r_{sv})_{pred}$ mg/cm³ · h
12.83	151.06	2.69	2.04	0.086	7.83	7.841
17.76	152.47	3.50	2.54	0.102	8.545	8.529
40.35	78.24	6.49	5.11	0.158	5.957	5.933
48.06	72.16	3.54	2.65	0.245	3.345	3.342

Diffusivity estimated from the best fit of the steady state biofilm kinetic model to the experimental specific biofilm degradation rates.

As shown in Table 3, the ratio of the diffusivities of phenol and oxygen within the biofilm to those in pure water, D_f/D_w, ranges from 8.6 to 24.5%, and appears to increase with decreasing biofilm density. Since in a biofilm with a higher density the number of cells and amount of exopolymer per unit biofilm volume would be higher, the tortuosity and the void in the biofilm could be expected to be higher and lower, respectively. Consequently, the resistance to diffusion of phenol and oxygen through the biofilm would be greater. The result of increasing diffusivity with decreasing biofilm density therefore appears to be reasonable. The numerical values of D_f/D_w obtained in this study, ranging from 8.6 to 24.5%, lie between the value of 8% obtained by Mueller et al. (1968) for self-aggregated bioflocs of *Zoogloea ramigera* and the value of 34% reported by Smith and Coackley (1984) for activated sludges thickened by centrifugation. Since the dry density of the biofilms attached to solid particles lies between that of the self-aggregated bioflocs and that of thickened sludges, the values of diffusivities of phenol and oxygen evaluated from the steady state biofilm model appear to be reasonable.

Zehner (1986) evaluated the diffusivity of phenol through the biofilm. Bioparticles obtained from the same DTFBR with biofilm thicknesses ranging from 6.9 to 41.2 μm were inactivated with $HgCl_2$ solution, then placed in a well-stirred tank in which the decay of phenol concentration with time was monitored. These data were fitted into the unsteady state mass balance equations to determine the only unknown parameter in the equations, i.e., the diffusivity of phenol within biofilm. The diffusivity thus obtained accounts for from 13 to 25% of that in pure water, very closely matching the estimated values obtained in this study. This finding strongly supports indirectly the validity of the proposed model for the DTFBR biofilm system.

It should be noted that the effective diffusivities of phenol and oxygen within the biofilm were examined under the conditions that the bulk phenol concentration S^b (ranging from 2.69 to 6.49 $\times 10^{-3}$ kg/m³) was significantly smaller than K_i (0.113 kg/m³), and that the bulk dissolved oxygen concentration C^b (ranging from 5.1 to 8.4 $\times 10^{-3}$ kg/m³) was far greater than K_{ox} (0.1×10^{-3} kg/m³). Under these conditions, the inhibitory effect of phenol was not present and the dependency of specific growth rate on oxygen was regarded as the zeroth order. The experimental data therefore actually tested the extreme situation of the model, Eqs. 6 and 7, i.e.,

$$\frac{D_{s,f}}{r^2}\left[\frac{\partial}{\partial r}\left(r^2\frac{\partial S}{\partial r}\right)\right] - \frac{\rho_v}{Y_{x/s}}\frac{\mu_{\max}S}{K_s + S} = 0 \tag{20}$$

$$\frac{D_{c,f}}{r^2}\left[\frac{\partial}{\partial r}\left(r^2\frac{\partial C}{\partial r}\right)\right] - \frac{\rho_v}{Y_{x/o}}\frac{\mu_{\max}S}{K_s + S} = 0 \tag{21}$$

However, the more generalized model propoed in this study—i.e., Eqs. 1, 2, and 6 to 11—is believed to be valid due to the mechanistic nature of the model and its verification for extreme cases.

Simulation

The numerical simulation based on the model at a range beyond the experimental conditions was carried out in this study with the following considerations.

1. The phenol content in surface water is regulated by the Environmental Protection Agency (EPA) to be less than 1.0×10^{-3} kg/m^3. At such low bulk phenol concentrations, the overall conversion rate for a completely mixed reactor such as the DTFBR is low. To treat wastewater containing high phenol concentration to meet the EPA requirement, either the residence time of wastewater in the reactor must be decreased (by decreasing the wastewater influent flow rate or by increasing the reactor volume), or the wastewater must be diluted before feeding into the reactor. Another alternative would be to use two-stage or multistage DTFBR's. Knowledge of the conversion rates of the biofilm systems in the DTFBR at a wide range of phenol concentration would provide the basic information for process optimization.

2. Oxygen has been observed to be one of the limiting factors in the treatment of phenol-containing wastewater in conventional and tapered three-phase fluidized-bed reactors at high biomass holdup (Holladay et al., 1978; Lee et al., 1979; Donaldson et al., 1984). Results of simulation based on the proposed bisubstrate-limiting kinetics would provide the oxygen requirement information for the DTFBR biofilm system used for aerobic wastewater treatment.

3. Simulation of the proposed model will give the general perspectives of the apparent kinetic behavior of a bisubstrate-limiting and substrate inhibitory immobilized cell system in a completely mixed reactor.

Simulations of the steady state operational performance of the DTFBR employed the values of biological and physical parameters, including biofilm thickness, biofilm dry density, biokinetic constants, particle diameter, and diffusivities of phenol and oxygen within the biofilm, obtained in three of the steady state experimental runs having biofilm thicknesses of 17.76, 40.35, and 48.06 μm, respectively. The volume fraction of the bare solid particles in the DTFBR was set to be the same for all three simulation runs. This fixed solid-loading condition corresponds to the routine operation of the fluidized-bed biofilm reactor in which the number of solid particles is maintained approximately constant. On this basis, the run that contains thicker biofilms would have higher biomass holdup in the reactor. The dimensionless biomass holdup, defined as $\rho_v[(1 + \delta/r_p)^3 - 1]\,\epsilon_s/(Y_{x/s}\sqrt{K_s K_i})$, for the three runs with biofilm thicknesses of 17.76, 40.35, and 48.06 μm are 0.5880, 0.7745, and 0.8859, respectively, for 20 vol. % solid loading. The dissolved oxygen concentration in the bulk liquid phase is assumed to remain constant at 6.0×10^{-3} kg/m^3.

Little has been studied on the liquid-solid mass transfer in a three-phase fluidized-bed reactor. Recently, Arters and Fan (1986) investigated the liquid-solid mass transfer in a conventional three-phase fluidized-bed reactor (CTFBR) (without a draft tube). Their results show that the liquid-solid mass transfer coefficient increases with increasing gas velocity and is independent of liquid velocity. A correlation equation was obtained that covers a wide range of gas and liquid velocities. One of the major differences in flow characteristics in a DTFBR from those in a CTFBR is the intensive circulative flow of liquid and bubbles between the draft tube and annular regions in the DTFBR. Under a low gas velocity, the bubbles do not completely penetrate through the annular region of the DTFBR. The deviation in the flow behavior in a DTFBR from that in a CTFBR due to gas effect would then become less significant. Since the liquid flow does not play a significant role in the liquid-solid mass transfer in a three-phase fluidized-bed, under a low gas velocity as encountered in this study the liquid-solid mass transfer coefficient predicted by the correlation equation of Arters and Fan (1986) for a CTFBR should provide a good approximation of the k_s value in a DTFBR. Calculation of the k_s using this correlation equation gives a value of 0.005 cm/s. The liquid-solid mass transfer coefficient in the 1,000 cm^3 DTFBR under the same operating conditions as those in the biodegradation processes was determined as 0.004 cm/s, based on the benzoic acid dissolution method presented by Tang et al. (1985). Comparison of the k_s value obtained experimentally in the DTFBR with that calculated using Arter and Fan's correlation equation shows that the experimental k_s of phenol for the DTFBR is reasonable. The external mass transfer coefficient of oxygen, k_c, was estimated from the value of k_s from the relationship:

$$\frac{k_c D_{s,w}}{k_s D_{c,w}} = \frac{2 + 0.95(\rho_\ell U d_f/\mu_\ell)^{0.5}(\mu_\ell/\rho_\ell D_{c,w})^{0.33}}{2 + 0.95(\rho_\ell U d_f/\mu_\ell)^{0.5}(\mu_\ell/\rho_\ell D_{s,w})^{0.33}} \tag{22}$$

extracted from the Garner-Suckling correlation equation for flow past a single sphere particle. The numeric values of all the parameters of the biofilm model used in the simulation are summarized in Table 4.

The performance of the DTFBR can be judged from its over-

Table 4. Values of Parameters in Biofilm Model Used in Simulation

$\mu_{\max}$	0.365	h^{-1}
K_s	10.948×10^{-3}	kg/m^3
K_i	113.004×10^{-3}	kg/m^3
K_{ox}	0.1×10^{-3}	kg/m^3
k_s	0.004	cm/s
k_o	0.0077	cm/s
$K_\ell a$	50.0	h^{-1}
$Y_{x/s}$	0.496	mg/mg
$Y_{x/o}$	0.354	mg/mg
$D_{s,f}$	varied	
$D_{c,f}$	varied	
ρ_v	varied	

all reactor conversion rate and the conversion fraction of substrates. Effects of substrate loading rates and bulk substrate concentration in dimensionless forms on reactor conversion efficiency are presented in the following discussion.

Figure 3 presents the relationship between the dimensionless reactor conversion rates and the dimensionless substrate loading rates with the dimensionless reactor biomass holdup as the parameter. As shown in this figure, for each run with different biomass holdups the dimensionless reactor conversion rate increases linearly with increasing dimensionless phenol loading rate until a certain maximum conversion rate is reached. The higher the total biomass holdup in the reactor, the higher the maximum conversion rate reached. It is noted that within a certain range of phenol loading rates more than one reactor conversion rate could exist corresponding to a given phenol loading rate, showing the possible existence of multiple steady states. This is further illustrated in Figure 4, which shows the variation of the outlet phenol concentration with inlet phenol concentration under steady state operation. It is seen that for a given biomass holdup and constant liquid inlet flow rate, there exists a certain range of inlet phenol concentrations in which three steady state outlet phenol concentrations correspond to a given inlet phenol concentration. The multiplicity of steady states is due to the nonlinear nature of the Haldane equation.

Figure 5 shows the variation of the dimensionless reactor conversion rates with the dimensionless bulk phenol concentrations. Since the maximum specific growth rate occurs at the phenol concentration equal to $\sqrt{K_s K_i}$ for Haldane-type growth kinetics, it can be expected that the maximum reactor conversion rates would be close to the dimensionless phenol outlet concentration equal to 1.0. The slight deviation is due to the existence of the concentration gradient within the biofilm.

The conversion fraction of phenol is plotted against the dimensionless phenol loading rate in Figure 6. In all three simulation runs the conversion fraction remains approximately between 0.98 and 0.99 for a range of phenol loading rates; it then decreases gradually with phenol loading rates. When the phenol loading rate reaches a certain value, the conversion fraction drops drastically with increasing phenol loading rates. The

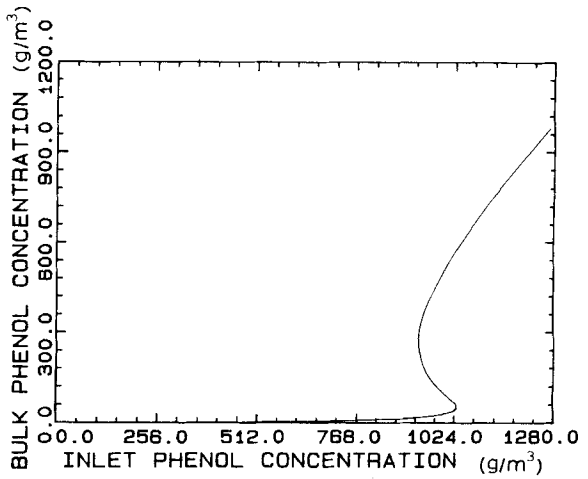

Figure 4. Inlet phenol concentration vs. corresponding outlet phenol concentrations in DTFBR.

Simulation run with dimensionless biomass holdup = to 0.5880, inlet liquid flow rate = 2,000 cm³/hr, reactor volume = 1,000 cm³

higher the biomass holdup is in the reactor, the larger the phenol loading rate will be before the conversion fraction begins to drop sharply.

Due to the diffusional resistance to substrates and oxygen transport within the biofilm, cells deep inside a very thick biofilm could be rendered inactive due to the deficiency in oxygen and/or substrates. Consequently, an optimal biofilm thickness and therefore an optimal biomass holdup could be expected. Beyond the optimal biofilm thickness, increase in biofilm thickness does not increase the active biomass, and the overall bioparticle density is reduced. Increase in the entrainment of bioparticles out of the reactor could result from the decrease in the overall density of the bioparticles. The optimal biofilm thickness in a liquid-solid fluidized-bed bioreactor has been identified by assuming a constant volume fraction of bioparticles and constant biofilm dry density and diffusivities of substrates and oxygen within the biofilm with respect to biofilm thickness (Kargi and Park, 1982; Shieh et al., 1981). However, it should be noted

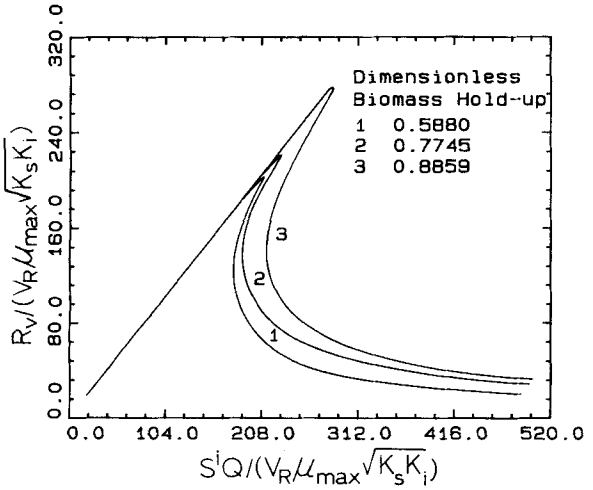

Figure 3. Dimensionless reactor conversion rates vs. dimensionless phenol loading rates for different dimensionless biomass holdups.

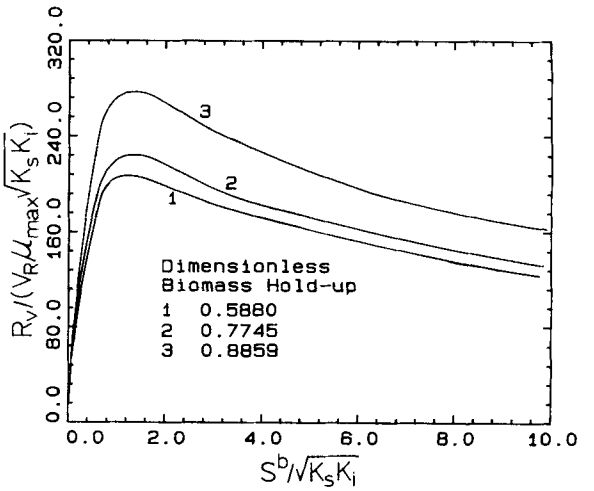

Figure 5. Dimensionless reactor conversion rates vs. dimensionless bulk phenol concentration for different dimensionless biomass holdups.

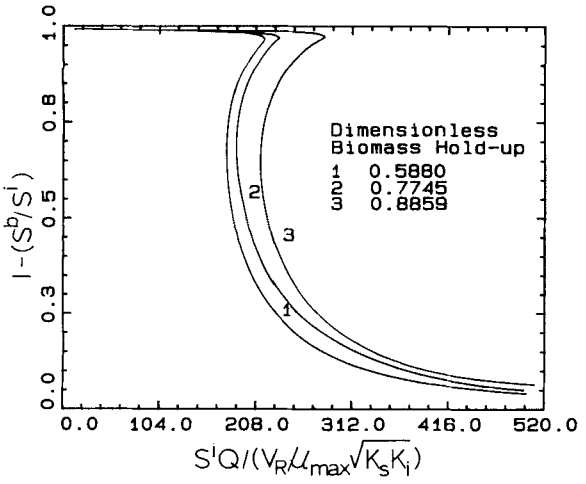

Figure 6. Phenol conversion fraction vs. dimensionless phenol loading rates for different dimensionless biomass holdups.

that the biofilm dry density varies with biofilm thickness and that the diffusivities of oxygen and substrates within the biofilm varies with biofilm dry density. As a result, quantitative expressions for the variation of biofilm dry density with biofilm thickness and for the variation of diffusivities of chemical species within the biofilm with biofilm dry density must be identified first to accurately predict the optimal biofilm thickness. In this study, data obtained are not sufficient to draw the conclusive quantitative relationships between the biofilm dry density and the biofilm thickness as well as between the diffusivities within the biofilm and the biofilm dry density. Consequently, the optimal biofilm thickness was not identified.

One of the major operating costs for aerobic fermentation or wastewater treatment is the energy cost for oxygenation of the system. Figure 7 presents the effect of bulk oxygen concentration on the overall reactor phenol biodegradation rate under different bulk phenol concentrations. It is shown in this figure that at a given bulk phenol concentration, the overall phenol biodegradation rate increases significantly only within a limited range of bulk oxygen concentrations. The requirement for oxygen to give a desired overall phenol biodegradation rate strongly depends upon the bulk phenol concentration to be maintained. Such information is important for the overall process optimization based on energy consumption.

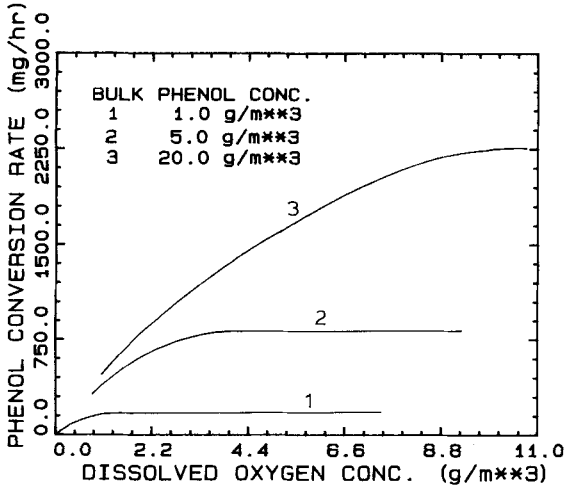

Figure 7. Effect of bulk dissolved oxygen concentration on reactor phenol conversion rate.
Simulation run with dimensionless biomass holdup = 0.5880

Concluding Remarks

The biofilms developed in the DTFBR have a biofilm dry density considerably higher than those cultivated in liquid-solid two-phase systems at a given biofilm thickness. A higher biomass holdup therefore can be achieved in the DTFBR than in the liquid-solid, two-phase fluidized-bed systems for a given biofilm thickness and a given solid particles loading. The biofilm dry density was found to vary with the biofilm thickness. Caution therefore needs to be exercised when extrapolated biofilm thicknesses are to be used in the simulation of a biofilm model and when biofilm growth is to be considered in unsteady state biofilm modeling.

The proposed steady state biofilm model in the DTFBR considers the simultaneous diffusion and reaction of both phenol and oxygen within the biofilms as well as the external mass transfer resistance between the biofilm surfaces and the completely mixed bulk liquid phase. The numerical values of the diffusivities of phenol and oxygen within the biofilm evaluated by the proposed biofilm model, ranging from 8.6 to 24.5% of those in water, are good estimates as compared with data reported in the literature. This indirectly verifies the biofilm model proposed in this study. Simulation results show that the steady state biofilm model provides a valuable tool to identify the optimal operating conditions for treatment of wastewater containing inhibitory organics in the draft-tube, three-phase fluidized-bed reactor.

Results of simulation employing the biofilm model indicate that the biomass holdup is the most critical factor for efficient performance of the DTFBR. Multiplicity of steady states can be encountered, based on the simulation results, at a certain range of high phenol loading rates in the DTFBR. These phenol loading rates at which multiple steady states occur depend upon the influent phenol concentration, the inlet liquid flow rate, and the biomass holdup in the reactor.

Acknowledgment

Financial support from the Office of Water Policy, U.S. Department of the Interior, under Grant No. CT 383700 is acknowledged.

Notation

A_b = overall surface area of bioparticles in reactor, m^2
C = dissolved oxygen concentration inside bioparticle, kg/m^3
C^b = dissolved oxygen concentration in bulk liquid, kg/m^3
C^s = dissolved oxygen concentration at biofilm surface, kg/m^3
C^* = dimensionless dissolved oxygen concentration inside biofilm
d_f = diameter of bioparticle, m
d_p = average diameter of solid particle, m
$D_{c,f}$ = diffusivity of oxygen within biofilm, m^2/h
$D_{c,w}$ = diffusivity of oxygen in pure water, m^2/h
D_f = diffusivity of a chemical species within biofilm, m^2/h
$D_{s,f}$ = diffusivity of phenol within biofilm, m^2/h
$D_{s,w}$ = diffusivity of phenol in pure water, m^2/h
D_w = diffusivity of a chemical species in pure water, m^2/h
k_c = solid-liquid phase mass transfer coefficient of oxygen, m/h
k_s = solid-liquid phase mass transfer coefficient of phenol, m/h
K_i = inhibition constant, kg/m^3
K_i^* = dimensionless inhibition constant

$K_L a$ = overall gas-liquid mass transfer coefficient, h^{-1}
K_{ox} = saturation constant of oxygen, kg/m^3
K^*_{ox} = dimensionless saturation constant of oxygen
K_s = saturation constant of phenol, kg/m^3
K^*_s = dimensionless saturation constant of phenol
N = total number of activated carbon particles in sample
Q = inlet liquid volumetric flow rate, m^3/h
r = radial position within bioparticle, m
r_f = radius of bioparticle, m
r_p = radius of activated carbon particle, m
r_{sv} = volumetric biofilm phenol degradation rate, defined as phenol degradation rate per unit volume of biofilm, $kg/m^3 \cdot h$
R_{ov} = overall reactor oxygen degradation rate, kg/h
R_v = overall reactor phenol degradation rate, kg/h
S = phenol concentration inside biofilm, kg/m^3
S^b = phenol concentration in bulk liquid, kg/m^3
S^i = inlet phenol concentration, kg/m^3
S^s = phenol concentration at biofilm surface, kg/m^3
S^* = dimensionless phenol concentration within biofilm
U = slip velocity of bioparticle, m/h
V_b = total biofilm volume in reactor, m^3
V_R = total reactor volume, m^3
W = dry weight of biomass in sample, kg
$Y_{o/s}$ = $g/O_2/g$ phenol consumed
$Y_{x/s}$ = growth yield coefficient of phenol
$Y_{x/o}$ = growth yield coefficient of oxygen

Greek letters

ξ = dimensionless radius of bioparticle
ξ^0 = dimensionless distance at biofilm surface
δ = thickness of biofilm, m
ϵ_g = volume fraction of gas in reactor
ϵ_ℓ = volume fraction of liquid in reactor
ρ_ℓ = density of liquid, kg/m^3
ρ_b = biofilm dry density, kg/m^3
μ_ℓ = viscosity of liquid, $kg/m \cdot s$
μ = specific growth rate, h^{-1}
μ_{max} = maximum specific growth rate, h^{-1}

Literature cited

Arters, D. C., and L.-S. Fan, "Solid-Liquid Mass Transfer in a Gas-Liquid-Solid Fluidized Bed," *Chem. Eng. Sci.*, **41,** 107 (1986).

Atkinson, B., J. D. Cunningham, and A. Pinches, "Biomass Holdups and Overall Rates of Substrate (Glucose) Uptake of Support Particles Containing a Mixed Microbial Culture," *Chem. Eng. Res. Des.*, **62,** 155 (1984).

Atkinson, B., and F. Mavituna, *Handbook of Biochemical Engineering,* Macmillan, London (1983).

Bailey, J. E., and D. F. Ollis, *Biochemical Engineering Fundamentals,* McGraw-Hill, New York (1977).

Beltrame, P., P. L. Beltrame, P. Cartini, and D. Pitea, "Kinetics of Phenol Degradation by Activated Sludges in a Continuous-Stirred Reactor," *J. Water Poll. Control Fed.*, **52,** 126 (1980).

Bungay, H. R., W. J. Whalen, and W. M. Sanders, "Microprobe Techniques for Determining Diffusivities and Respiration Rates in Microbial Slime Systems," *Biotechnol. Bioeng.*, **11,** 765 (1969).

D'Adamo, P. D., A. F. Rozich, and A. F. Gaudy, Jr., "Analysis of Growth Data with Inhibitory Carbon Sources," *Biotechnol. Bioeng.*, **26,** 397 (1984).

Donaldson, T. L., G. W. Strandberg, J. D. Hewitt, and G. S. Shields, "Biooxidation of Coal Gasification Wastewaters," *Environ. Prog.*, **3**(4), 248 (1984).

Dunn, I. J., H. Tanaka, S. Uzman, and M. Denac, "Biofilm Fluidized-Bed Reactors and Their Application to Wastewater Nitrification," *Ann. NY Acad. Sci.*, **413,** 168 (1983).

Fan, L.-S., K. Fujie, and T.-R. Long, "Some Remarks on Gas-Liquid Mass Transfer and Biological Phenol Degradation in a Draft-Tube, Gas-Liquid-Solid Fluidized-Bed Bioreactor," *AIChE Symp. Ser. No. 241,* **80,** 102 (1984).

Fan, L.-S., S.-J. Hwang, and A. Matsuura, "Hydrodynamic Behavior of a Draft-Tube, Gas-Liquid-Solid Spouted Bed," *Chem. Eng. Sci.*, **39,** 1677 (1984).

Hill, G. A., and C. W. Robinson, "Substrate Inhibition Kinetics: Phenol Degradation by *Pseudomonas putida,*" *Biotechnol. Bioeng.*, **17,** 1599 (1975).

Hoehn, R. G., and A. D. Ray, "Effects of Thickness on Bacterial Film," *J. Water Poll. Control Fed.*, **45,** 2302 (1973).

Holladay, D. W., C. W. Hancher, C. D. Scott, and D. D. Chilcote, "Biodegradation of Phenolic Waste Liquors in Stirred-Tank, Packed-Bed, and Fluidized-Bed Bioreactors," *J. Water Poll. Control Fed.*, **50,** 2573 (1978).

Hwang, S.-J., and L.-S. Fan, "Solid-Liquid Mass Transfer in a Draft-Tube, Gas-Liquid-Solid Spouted Bed," 16th Ann. Meet. Fine Particle Soc., Miami Beach (Apr. 1985).

Jennings, P. A., V. L. Snoeyink, and E. S. K. Chian, "Theoretical Model for a Submerged Biological Filter," *Biotechnol. Bioeng.*, **18,** 1249 (1976).

Jones, G. L., F. Jansen, and A. J. McCay, "Substrate Inhibition of the Growth of Bacterium NCIB 8250 by Phenol," *J. General Microbiol.*, **74,** 139 (1973).

Kargi, F., and J. K. Park, "Optimal Biofilm Thickness for Fluidized-Bed Biofilm Reactors," *J. Chem. Tech. Biotechnol.*, **32,** 744 (1982).

Klein, J., U. Hackel, and F. Wagner, "Phenol Degradation by *Candida tropicalis* Whole Cells Entrapped in Polymeric Ionic Networks," *Immobilized Microbial Cells, ACS Symp. Ser. No. 106,* Am. Chem. Soc., Washington, DC (1979).

Kubota, H., K. Fujie, and T. Kasakura, "Automatic Monitoring of Exhaust Gas Analysis in Activated Sludge Wastewater Treatment Process," *Water Sci. Technol.*, **13,** 159 (1981).

Lee, D. D., C. D. Scott, and C. W. Hancher, "Fluidized-Bed Bioreactor for Coal Conversion Effluents," *J. Water Poll. Control Fed.*, **51,** 974 (1979).

Matson, J. V., and W. G. Characklis, "Diffusion into Microbial Aggregates," *Water Res.*, **10,** 877 (1976).

Mueller, J. A., W. S. Boyle, and E. N. Lightfoot, "Oxygen Diffusion through Zoogloeal Flocs," *Biotechnol. Bioeng.*, **10,** 331 (1968).

Mulcahy, L. T., W. K. Shieh, and E. J. Lamotta, "Simplified Mathematical Models for a Fluidized-Bed Biofilm Reactor," *AIChE Symp. Ser. No. 209,* **77,** 273 (1981).

Park, Y., M. E. Davis, and D. A. Wallis, "Analysis of a Continuous, Aerobic, Fixed-Film Bioreactor. I: Steady State Behavior," *Biotechnol. Bioeng.*, **26,** 457 (1984).

Pawlowsky, V., and J. A. Howell, "Mixed Culture Biooxidation of Phenol. I: Determination of Kinetic Parameters," *Biotechnol. Bioeng.*, **15,** 889 (1973).

Powell, M. J. D., "A Hybrid Method for Nonlinear Equations," *Numerical Methods for Nonlinear Algebraic Equations,* P. Rabinowitz, ed., Gordon and Breach, London (1970a).

Powell, M. J. D., "A FORTRAN Subroutine for Solving Systems of Nonlinear Algebraic Equations," *Numerical Methods for Nonlinear Algebraic Equations,* P. Rabinowitz, ed., Gordon and Breach, London (1970b).

Rittmann, B. E., and P. L. McCarty, "Evaluation of Steady State Biofilm Kinetics," *Biotechnol. Biogen.*, **22,** 2359 (1980).

Scott, D. S., and C. W. Hancher, "Use of a Tapered Fluidized Bed as a Continuous Bioreactor," *Biotechnol. Bioeng.*, **18,** 1393 (1976).

Shieh, W. K., "Suggested Kinetics Model for the Fluidized-Bed Biofilm Reactor," *Biotechnol. Bioeng.*, **22,** 667 (1980).

Shieh, W. K., P. M. Sutton, and P. Kos, "Predicting Reactor Biomass Concentration in a Fluidized-Bed System," *J. Water Poll. Control Fed.*, **53,** 1574 (1981).

Smith, P. G., and P. Coackley, "Diffusivity, Tortuosity and Pore Structure of Activated Sludge," *Water Res.*, **18,** 117 (1984).

Standard Methods for the Examination of Water and Wastewater, 14th ed., Am. Pub. Health Ass., New York (1975).

Stathis, T. C., "Fluidized Bed for Biological Wastewater Treatment," *J. Environ. Eng. Div.*, 227, (Feb., 1980).

Suzuki, M., S. Momonoi, and H. Harada, "Phenolic Wastewater Treatment in Loop-type Bioreactor," *Proc. Symp. Biol. Wastewater Treatments,* Soc. Chem. Eng. Japan, Sandi, Japan, 34 (1983).

Szetela, R. W., and T. Z. Winnicki, "A Novel Method for Determining the Parameters of Microbial Kinetics," *Biotechnol. Bioeng.*, **23,** 1485 (1981).

Tang, W.-T., K. Wisecarver, and L.-S. Fan, "Reactor Dynamics of a

Draft-Tube, Fluidized-Bed Bioreactor Using Activated Carbon with Immobilized Living Cells," AIChE Ann. Meet., Chicago (Nov., 1985) Chem. Eng. Sci., in press (1987).
Timmermans, P., and A. Van Haute, "Influence of the Type of Organisms on the Biomass Holdup in a Fluidized-Bed Reactor," *Appl. Microbiol. Biotechnol.*, **19,** 36 (1984).
Wang, S-C. P., and T. Chi, "Bilayer Film Model for the Interaction between Adsorption and Bacterial Activity in Granular Activated Carbon Columns," *AIChE J.*, **30,** 786 (1984).
Williamson, K., and P. L. McCarty, "A Model of Substrate Utilization by Bacterial Films," *J. Water Poll. Control Fed.*, **48,** 9 (1976).
Yang, R. D., and A. E. Humphrey, "Dynamic and Steady State Studies of Phenol Biodegradation in Pure and Mixed Cultures," *Biotechnol. Bioeng.*, **17,** 1211 (1975).
Ying, W. C., and W. J. Weber, Jr., "Biophysicochemical Adsorption Model Systems for Wastewater Treatment," *J. Water Poll. Control Fed.*, **51,** 2661 (1979).
Zehner, B. J., "The Diffusivity of Phenol within a Fixed Microbial Film in a Draft-Tube, Three-Phase Fluidized-Bed Bioreactor," MS Thesis, Ohio State Univ. (1986).

Manuscript received Oct. 2, 1985, and revision received July 23, 1986.